

Turbulent Dynamics in Active Solids

Wilhelm Sunde Lie, Ingve Simonsen and Paul Gunnar Dommersnes*

Department of Physics, NTNU – Norwegian University of Science and Technology, Trondheim, Norway

(Dated: October 6, 2025)

We investigate numerically the polar ordering dynamics in the active elastic solid model (AES) and find classic signatures of turbulent dynamics: power-law scaling for the energy spectrum and non-Gaussian statistics of velocity increments. However, there is no energy cascade, in line with previous findings for active turbulence in fluids. The results extend the concept of active turbulence to solid systems and are expected to be important for understanding active biological solids, such as bacterial colonies and migrating epithelial monolayers.

Introduction — Active fluids has become a broad field within non-equilibrium physics, including many topics such as phase transitions, liquid crystals, topological defects, active sound, and active turbulence [1–3]. The theories developed for active fluids clearly impact how we think about and understand cell biology. Active fluids can also solidify and turn into active solids. Numerical particle models show that active matter systems can undergo fluid-solid phase transitions [4–7]. There is also growing evidence that fluid-solid transitions of cell tissues play a central role in developmental biology [8, 9]. Epithelial cell layers has been shown to act as active solid sheets that can pulsate internally or self-propel on a substrate [10–13]. The development of active solids theories is also naturally linked to adaptive and self-organizing robotic systems [14, 15].

Recently there has been renewed interest in the Active Elastic Solid Model (AES) [16, 17], which is a simple particle model of a two-dimensional self-propelled solid, that may for example represent a solid monolayer of cells crawling on a surface. The particles are held together by linear elastic springs, and the propulsion direction of the particles align with the direction of the elastic forces that act on them. This mechanism is also called “self-alignment” as particles align in the direction of their local velocity field [18]. The self-alignment mechanism in the AES model is conceptually different from the Vicsek swarm model, where particles align propulsion direction according to the propulsion direction of their neighbors [19]. The difference between these two alignment mechanisms is particularly clear in solids, whereas polarity-polarity coupling would yield a linear diffusive polar dynamics in a solid, the AES force-alignment mechanism is nonlinear. More recently it has been found that the AES model exhibit many interesting and unique features that are of relevance to cell biology. It was shown both theoretically and in the case of synthetic active matter that force alignment results in nonlinear rotational polarity oscillations in confined active solids [21, 22]. Solid bacterial films show exactly the same behavior with self-sustained rotating and oscillation modes that seems to be very well described by the AES model [20]. In vitro

experiments show that epithelial cells form solid monolayers that behave as oscillating or self-propelled solid sheets on a substrate [11–13], the polar ordering dynamics included contractive elastic topological defects that again seem to agree well with simulations of the AES model [12].

Active fluids like swimming bacterial colonies or motile epithelial cell layers exhibit vortices of swirling motion and power law distributed energy spectrum, known as active turbulence [2, 3, 23]. The framework of turbulent dynamics has also been employed in visco-elastic polymer systems, where it is called “elastic turbulence” [25]. This suggest investigating the dynamics of the AES model from a turbulent dynamics perspective. The type of turbulence we here refer to is somewhat different from steady-state turbulence usually studied in active fluids, we are rather interested in the transient dynamics of ordering, starting from an initially disordered state that evolves into global large-scale motion. It may be considered to be within the same class of phenomena as freely developing turbulence, such as classical two-dimensional inertial turbulence that evolves from initially small vortices that merge into larger vortices and form a transient scale-invariant velocity field [26]. A similar type of developing turbulence has also been found in polar active fluids [27]. Notice that our motivation for studying this ordering dynamics comes from experiments on solid epithelial monolayers [12], where the polar ordering process takes about one day for an epithelial patch of radius 1 cm. It is therefore of practical importance to understand the underlying mechanisms that drive polar ordering.

The active elastic solid model (AES) in its simplest form [16, 21] is given by the coupled dynamics of particle positions and particle polarity:

$$\zeta \partial_t \mathbf{r}_i = \mathbf{F}_i + F_a \mathbf{p}_i \quad (1)$$

$$\partial_t \mathbf{p}_i = -\xi \mathbf{p}_i \times (\mathbf{p}_i \times \mathbf{F}_i) \quad (2)$$

where, for particle i , \mathbf{r}_i is its position vector, and $\mathbf{p}_i = (\cos \theta_i, \sin \theta_i)$ is its polarity vector (propulsion direction). The vector \mathbf{F}_i is the sum of elastic forces acting on particle i from the neighboring particles $-K(d_{ij} - r_{ij})\hat{\mathbf{r}}_{ij}$, where d_{ij} is the equilibrium distance between the particle i and its neighbor j . The constant F_a is the magnitude of the propulsion force, and ζ is a friction coefficient, or inverse mobility coefficient. Equation (1) asserts that the

* contact author: paul.dommersnes@ntnu.no

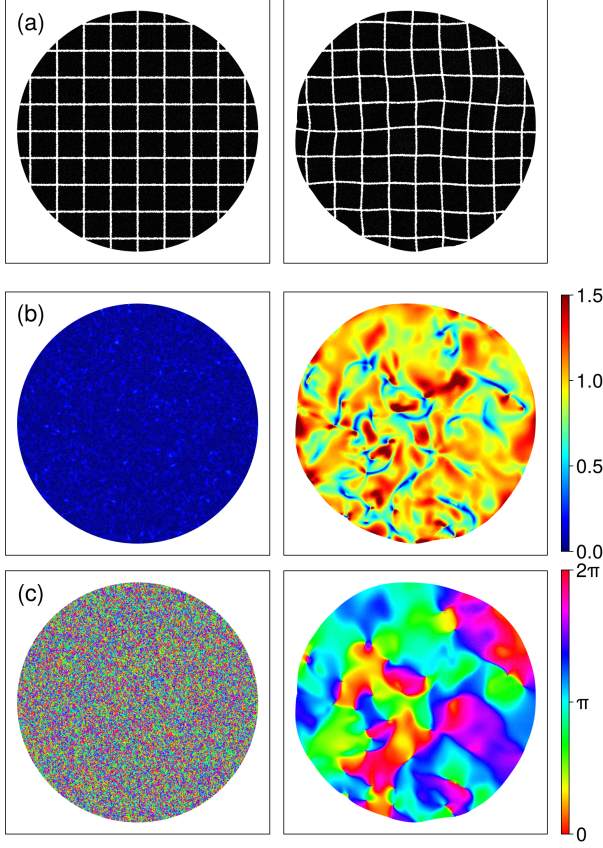


FIG. 1. (a) Elastic deformations, at start of simulation (left) and during ordering process (right). (b) Magnitude of the velocity field at start (left) and during ordering (right). (c) Direction of the velocity field. Parameters: $N = 128\,000$, $K = 20$, $\xi = 6$. The left column corresponds to the early stage with no net polar order $\Pi = 0.0$. In the right column, the system has a global polar order of $\Pi = 0.25$.

speed of the particle in the absence of external forces is constant $V_a = F_a/\zeta$, and the velocity is either slowed down or increased due to external elastic forces acting on the particle. Equation (2) asserts that the polarity aligns in the direction of the total elastic force acting on the particle, with a turning rate ξ . This term is mathematically equivalent to the damping term in the ferromagnetic Landau-Lifshitz equation, one may thus think of the force field as equivalent to a magnetic field that orients spins in a solid. Notice that in Eq. (2) one could also replace the elastic force by \mathbf{F}_i by $\zeta\partial_t\mathbf{r}_i$, i.e. polar alignment with elastic forces is equivalent to polar alignment with particle velocity [18].

Adding sufficient noise in the AES model results in loss of polar order through a second order phase transition [16, 24], here we choose to focus on the noise-less model, and understand the chaotic dynamics resulting from the active forces in the AES model. This is in line with the approach to active turbulence in noiseless

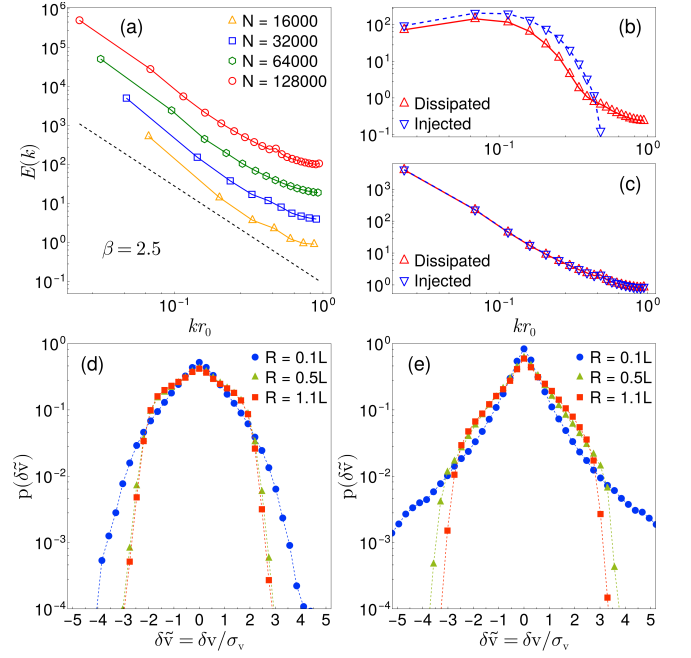


FIG. 2. (a) Energy-spectra (at $\Pi = 0.7$) show broad distribution over length-scales. (b) At very early stages injection spectrum and dissipation spectrum are different, however (c) shows that the system evolve towards a situation where dissipation and injection of energy is balanced on all scales. (d) Velocity increment at $\Pi = 0.1$ shows some Gaussian-like behavior on short scales. (e) As the systems evolve to $\Pi = 0.7$ there is a strong non-Gaussian velocity fluctuation on intermediate scales. Parameters for (a)–(e): $N = 128\,000$, $K = 20$, $\xi = 4$. Figures (a)–(e) are ensemble average results.

nematic fluids [28].

Setup — The AES model is effectively a two-parameter model: rescaling length with the distance b between nearest-neighbor particles $\mathbf{r} = \tilde{\mathbf{r}}b$, and time $t = \zeta b\tilde{t}/F_a$, results in an effective dimensionless rigidity $\tilde{K} = Kb/F_a$ and dimensionless turning rate $\tilde{\xi} = \xi K F_a/\zeta$. This amounts to setting $\zeta = 1$ and $F_a = 1$ in the AES equations. In the following it is understood that K and ξ are measured in these units. We here simulate the particle AES model by direct integration of the coupled Eqs.(1) and (2) starting from an initial state where polarity vectors of each particle was set in random directions. In an experimental system this would corresponds to where cells are awakened from a quiescent state by serum [12]. The spring constant is set to $K = 20$, and we considered turning rates in the range: $\xi = 2$ –25. This ensures that the elastic deformations are not too large, and the linear spring model is reasonable. For $\xi < 1$, the ordering dynamics is too slow and larger stress builds up, we therefore do not consider that range here. Notice that it is straightforward to add non-linear elastic springs in this model [12], however we choose to work with linear spring elasticity to clarify that the non-linear dynamics arises solely from the polarity-force coupling. The AES model

was first defined on a hexagonal bead-spring lattice [16], however since our study was originally motivated by understanding epithelial cell layers [12] we chose to work with a statistically isotropic lattice bead-spring network. The network is created by first performing Langevin simulation of growing beads that form a disordered solid. The final bead diameters is heterogeneous and uniformly distributed in the range $b \in [0.85, 1.15]$. The beads centers are then connected by Voronoi tessellation, similar to reference [12, 29]. The result is a heterogeneous network that is structurally isotropic on large scales (supplemental material). We chose to work with circular patches, with free boundary conditions. This allows for spontaneous symmetry breaking of the final polarization direction. Imposing boundary conditions is also possible, but can result in more complex dynamics due the final state having oscillatory or unsteady dynamics.

Results — In the initial stage of the ordering process the particles move in random directions, which results in a quite rapid buildup of elastic forces. Small domains of polar order start to grow, which forces other particles to align. The polar order is measured by: $\Pi = |\sum_{i=1}^N \mathbf{p}_i|/N$.

At the start of the simulation $\Pi = 0$ and perfect order $\Pi \approx 1$ is always achieved at long times. The final ordered state is moving in a straight line with little fluctuations. The ordering process is however not a regular coarsening process, the polar order parameter evolves in a non-monotonous and intermittent manner (supplemental Figs. 8–9). The elastic deformations of the solid are quite weak throughout the whole ordering process, as shown in Fig. 1a, and would hardly evoke turbulent dynamics. However, the velocity field varies strongly both in direction and magnitude during the ordering process, as shown in Figs. 1b and 1c. The velocity vorticity field shows a broad variation of structures from small to large scales, reminiscent of turbulent structures (Fig. 3a). Notice, however, that the vorticity map exhibits more string-like structures than vortices, which means that the velocity field is dominated by fronts of sudden change of velocity, a kind of domain walls, which appear very clearly in the angular velocity field (time derivative of velocity direction), Fig. 3d. A very similar domain wall structure was also found experimentally in solid epithelial cells during ordering [12].

In active fluid turbulence one defines an “energy” [2, 3]: $E = \int d^2r \mathbf{v}^2/2$. The inertial kinetic energy does not play a direct role in these systems; this velocity square field is rather a measure of activity in a region in space. For example some regions are jammed with frustrated orientation of cells pushing against each other, whereas others exhibit coherent motion. The velocity energy spectrum $\mathcal{E}(k)$ is defined by: $E = \int dk \mathcal{E}(k)$ where k is the wave number. In a system with turbulent dynamics one expects a scale-free spectrum $\mathcal{E}(k) \sim 1/k^\beta$. We find that the AES model display such a broad distribution of energy over length-scales, with an exponent of approximately $\beta \approx 2.5$, as shown in Fig. 2a. These energy

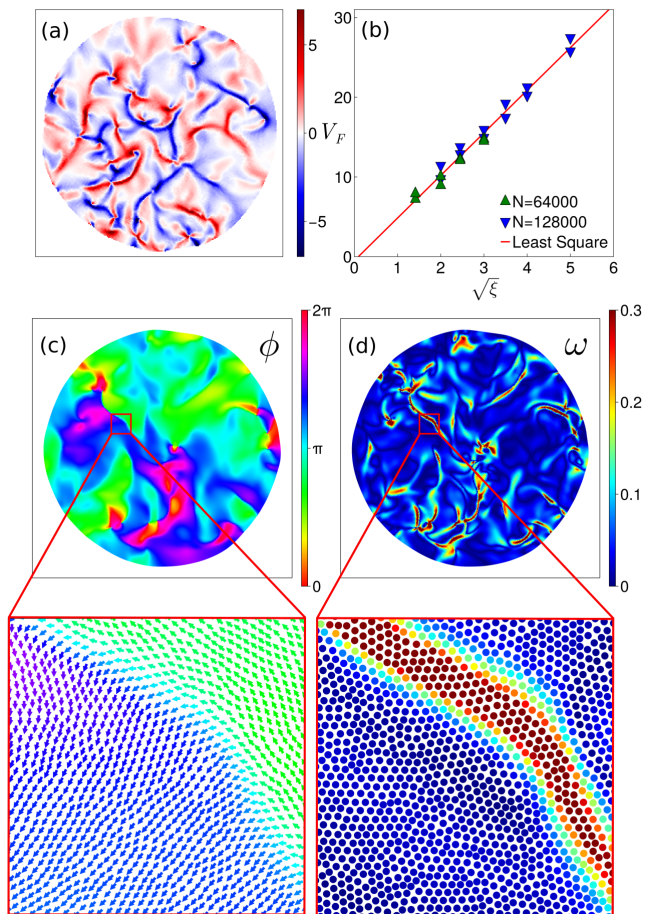


FIG. 3. (a) Vorticity map of a snapshot of the velocity field in a system with parameters $N = 128\,000$, $K = 20$, $\xi = 6$, and an ordering $\Pi = 0.25$. (b) Velocity of domain walls V_F for different turning rates ξ . The markers are individual measurements from systems the systems, green originating from systems of $N = 64\,000$ particles, while blue markers are from systems of $N = 128\,000$ particles. (c) Direction of velocity field with cutout displaying a domain wall. (d) Angular velocity of the velocity direction displaying high angular velocity at the domain wall.

spectra are obtained by ensemble averaging.

In inertial hydrodynamic turbulence it is well known that energy is transferred between different length-scales, this is not necessarily the case in active turbulent systems, in turbulent active nematic the active work is dissipated on the scale in which it is injected [3]. We follow [3] and define an injection spectrum from the work produced by active forces: $\int d^2r F_a \mathbf{p} \cdot \mathbf{v}$, and a dissipation spectrum from $\int d^2r \zeta \mathbf{v} \cdot \mathbf{v}$. We find that in the very early dynamics there a difference between these spectra (Fig. 2b), indicating initial transfer of energy between scales, however as the system develops the two distributions become near identical (Fig. 2c), indicating that energy is dissipated at the scale it is injected, *i.e.* there is no storage of elastic energy that is transmitted between different length-scales.

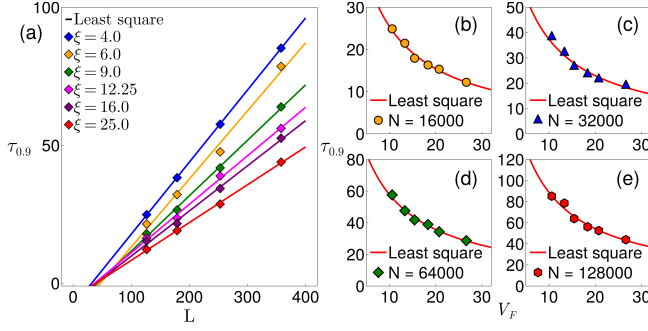


FIG. 4. (a) Ensemble results for the time to order $\tau_{0.9}$ against the system size L , for different turning rates ξ . Data points are accompanied by lines fitted using the least squares method. (b)–(e) Ensemble results for the time to order $\tau_{0.9}$ against the velocity of domain walls V_F . Data points are accompanied by inverse linear, least squares fitted functions, fitted to $\tau_{0.9}^{-1}$.

A second important feature that is commonly used to characterize inertial hydrodynamic turbulence is intermittency, *i.e.* sudden bursts of motion, which can be quantified by the probability distribution of the longitudinal velocity increments.

$$\delta v_{||} = [\mathbf{v}(\mathbf{r} + \mathbf{R}) - \mathbf{v}(\mathbf{r})] \cdot \hat{\mathbf{R}} \quad (3)$$

where $R = |\mathbf{R}|$ is the distance at which velocities are compared. In inertial hydrodynamic turbulence the velocity increments are found to be non-Gaussian (broad distributions) when R is an intermediate scales, and they become Gaussian on larger scales. Such non-Gaussian velocity increments have also been observed in turbulent dynamics in granular media [31]. We find that the AES model also exhibit clear non-Gaussian velocity increments, the broadening becomes more pronounced as the system evolves towards intermediate polar order, as can be seen in Fig. 2e).

The AES model thus exhibits the main characteristic of turbulent dynamics, scale-free energy spectra and non-Gaussian statistics for velocity increments. However the velocity field is not like the swirling vortices seen in inertial or active fluid turbulence (which would be hard to imagine in a solid), the dynamics is rather dominated by velocity domain walls, *i.e.* lines of sudden change in velocity (and polarity), as seen in Fig. 1 and Fig. 3a. We observed in simulations that these walls move rapid through the system at a speed that exceeds the propulsion speed of particles. Although this front velocity is not necessarily what drives the turbulent dynamics, it seems to be central in the dynamics. Scaling analysis of the continuum AES equations reveals a characteristics speed, $V_F = (\xi K F_a / \zeta)^{1/2}$ where K now is the macroscopic elastic constant (see supplemental information). Numerical tracking of domain walls indeed show that their velocities on average follow a square root dependence: $V_F \sim \sqrt{\xi}$, as shown in Fig. 3b.

The time to produce almost perfect polar order in the

system scales linearly with system size L , as seen in Fig 4a. Notice that a similar observation was reported in Ref. 17 for smaller systems. This suggest a scaling relation $\tau \sim L/V_F$, *i.e.* that the ordering time is controlled by speed of domain walls.

It is possible that one could consider the active solid turbulence as a kind of wave-turbulence, *i.e.* domain walls of polarity that move and collide. This behavior also highlights the difference with Vicsek-Toner-Tu type polarity coupling which would result in a linear diffusive dynamics in the solid: $\partial_t \mathbf{p} = \lambda \nabla^2 \mathbf{p}$ and hence a diffusive ordering time for reaching polar order $\tau \sim L^2$. This suggest that the AES turbulent dynamics would be a more effective mean of collective ordering for cells than polarity-polarity coupling.

It is not clear how the results apply to periodic boundary conditions (as is often used in active turbulence), since it would impose a global compression constraint that might reduce fluctuations, the free boundaries we use here allow global area fluctuations of the patch.

In inertial turbulence the Reynolds number controls the transition from laminar to turbulent flow. Transition from ordered flow to turbulence is also known to occur in active fluid turbulence [3, 30]. Although we did not explore all parameter space, we did not see any sign of a transition in the dynamics. This might have a natural explanation, there is no equivalent of viscosity in the AES model, *i.e.* a terms that smoothen the polarity or velocity field. It is possible to combine self-alignment with Vicsek alignment, which gives diffusive (viscosity like smoothing term) Toner-Tu in combination with the self-alignment term [32], which might result in a transition between diffusive coarsening dynamics and turbulent dynamics.

We have shown that the transition to polar order in the AES model can be considered as a turbulent fluctuation, exhibiting power law scaling and non-Gaussian velocity increments. Rather than vortices like in hydrodynamic turbulence, the dynamics of the active solid velocity field is dominated by fronts of sudden change of velocity, that propagate through the system at speeds much higher than the maximum propulsion speed of particles. Since our system is free (no boundaries) it eventually evolves into perfect order. There appears to be no equivalent to an energy cascade in the system. In epithelial cell monolayers one would expect some non-linear elasticity, including this in the model can give an alternative mechanism of non-linear transfer of energy between scales, and possibly lead to an elastic energy cascade in the system. The predictions and analysis presented here could be pursued in experiments on solid motile polar cell layers, or in synthetic active matter system with a large number of particles.

ACKNOWLEDGMENTS

P.G.D. thanks E. Lång, A. Lång, S. O. Bøe and F. Brochard-Wyart for discussions on solid cell dynamics. We thank L. Fleinghaus, M. Nytttingnes, H. H. Haavind,

T.K. Pedersen and C. Aarset Nygård for many discussions on the AES model. We thank J.-F. Joanny for discussions and helpful suggestions on the manuscript. The simulations were performed on the Hemmer computer cluster, Department of Physics, NTNU.

-
- [1] M. C. Marchetti, J. F. Joanny, S. Ramaswamy, T. B. Liverpool, J. Prost, Madan Rao, and R. Aditi Simha, *Rev. Mod. Phys.* **85**, 1143 (2013).
 - [2] H. H. Wensink, J. Dunkel, S. Heidenreich, K. Drescher, R. E. Goldstein, H. Löwen, and J.-M. Yeomans, *Proc. Nat. Acad. Sci.* **109**, 14308–14313 (2012).
 - [3] R. Alert, J. Casademunt, J.-F. Joanny, *Ann. Rev. Condens. Matter Phys.* **13**, 143–170 (2022).
 - [4] P. Digregorio¹, D. Levis, A. Suma, L. F. Cugliandolo, G. Gonnella, and I. Pagonabarraga, *Phys. Rev. Lett.* **121**, 098003 (2018).
 - [5] S. Henkes, Y. Fily, and M. Cristina Marchetti, *Phys. Rev. E* **84**, 040301(R) (2011).
 - [6] M. E. Cates and J. Tailleur, *Ann. Rev. of Condens. Matter Phys.* **6**, 219–244 (2015).
 - [7] G. S. Redner, M. F. Hagan, and A. Baskaran, *Phys. Rev. Lett.* **110**, 055701 (2013).
 - [8] A. Mongera et al., *Nature* **561**, 401–405 (2018).
 - [9] M. Popović, V. Druelle, N. A. Dye, F. Jülicher and Matthieu Wyart, *New J. Phys.* **23**, 033004 (2021).
 - [10] S. Armon, M. S. Bull, A. Moriel, H. Aharoni and M. Prakash, *Commun. Phys.* **4**, 216 (2021).
 - [11] K. Doxzen, S. R. K. Vedula, M. C. Leong, H. Hirata, N. S. Gov, A. J. Kabla, B. Ladoux B, and C. T. Lim, *Integr. Biol. (Camb)* **5**, 1026–1035 (2013).
 - [12] E. Lång, A. Lång, U. Blicher, P. R. Rognes, P. G. Dommersnes, S. O. Bøe, *Sci. Adv.* **10**, 1–14, (2024).
 - [13] Y. Shen, J. O’Byrne, A. Schoenit, A. Maitra, R.-M. Mège, R. Voituriez, B. Ladoux, *Proc. Nat. Aca. Sci.* **122**, (16) e2421327122 (2025).
 - [14] J. Veenstra, C. Scheibner, M. Brandenbourger, J. Binysh, A. Souslov, V. Vitelli and C. Coulais, *Nature* **639**, 935–941 (2025).
 - [15] B. Saintyves, M. Spenko, H. M. Jaeger, *Sci. Robot.* **9**, eadh4130 (2024).
 - [16] E. Ferrante, A. E. Turgut, M. Dorigo, and C. Huepe, *Phys. Rev. Lett.* **111**, 268302 (2013).
 - [17] E. Ferrante, A. E. Turgut, M. Dorigo, and C., Huepe, *New J. Phys.* **15**, 095011 (2013).
 - [18] P. Baconnier, O. Dauchot, V. Démery, G. Düring, S. Henkes, C. Huepe, and A. Shee, *Rev. Mod. Phys.* **97**, 015007 (2025).
 - [19] T. Vicsek, A. Czirók, E. Ben-Jacob, I. Cohen, and O. Shochet, *Phys. Rev. Lett.* **75**, 1226 (1995).
 - [20] H. Xu, Y. Huang, R. Zhang, and Y. Wu, *Nat. Phys.* **19**, 46–51 (2023).
 - [21] P. Baconnier et al. *Nat. Phys.* **18**, 1234–1239 (2022).
 - [22] Y. Kinoshita, N. Uchida, and A. M. Menzel, *J. Chem. Phys.* **162**, 054906 (2025).
 - [23] C. Blanch-Mercader, V. Yashunsky, S. Garcia¹, G. Duclos, L. Giomi, and P. Silberzan, *Phys. Rev. Lett.* **120**, 208101 (2018).
 - [24] M. Musacchio, A. P. Antonov, H. Löwen, and L. Caprini, *arXiv:2506.12967v1 [cond-mat.soft]* 15 Jun 2025.
 - [25] A. Groisman and V. Steinberg, *Nature* **405**, 53–55 (2000).
 - [26] J. Paret and P. Tabeling, *Phys. Rev. Lett.* **79**, 4162 (1997).
 - [27] N. Rana and P. Perlekar, *Phys. Rev. E* **102**, 032617 (2020).
 - [28] R. Alert, J.-F. Joanny, and J. Casademunt, *Nat. Phys.* **16**, 682–688 (2020).
 - [29] S. Soumya, A. Gupta, A. Cugno, L. Deseri, K. Dayal, D. Das, S. Sen, and M. M. Inamdar, *PLOS Comput. Biol.* **11**, e1004670 (2015).
 - [30] A. Doostmohammadi, T. N. Shendruk, K. Thijssen, and J. M. Yeomans, *Nat. Commun.* **8**, 15326 (2017).
 - [31] F. Radjai and S. Roux, *Phys. Rev. Lett.* **89**, 064302 (2002).
 - [32] H. Reinken and A. M. Menzel, *arXiv:2502.06312v1 [cond-mat.soft]* 10 Feb 2025.